DOE/ET-53088-328 IFSR #328

Effect of Scalar Nonlinearity on the Dipole Vortex Solution

X. Su, W. Horton, P.J. Morrison
Institute for Fusion Studies
The University of Texas at Austin
Austin, Texas 78712
and
V.P. Pavlenko
Institute for Nuclear Physics
Kiev, USSR

July 1988

Effect of Scalar Nonlinearity on the Dipole Vortex Solution

X. Su, W. Horton, P.J. Morrison
Department of Physics and Institute for Fusion Studies
The University of Texas at Austin
Austin, Texas 78712
and
V.P. Pavlenko
Institute for Nuclear Physics
Kiev, USSR

Abstract

The dipole vortex solutions of the Hasegawa-Mima drift wave or equivalently, the quasi-geostrophic Rossby wave equation are shown to be split up into long-lived monopole vortices (cyclones and anticyclones) in the presence of a small scalar, i.e. KdV type, nonlinearity. The lifetime of the dipole vortex varies inversely with the strength of the scalar nonlinearity.

I. Introduction

It is well known that the dipole vortex is an exact solitary wave solution to the dissipationless Hasegawa-Mima drift wave equation, which in the fluid mechanics literature is referred to as the Rossby wave equation

$$(1-\nabla^2)\frac{\partial\varphi}{\partial t}+v_d\frac{\partial\varphi}{\partial y}-[\varphi,\nabla^2\varphi]=0 \tag{1}$$

where

$$[\varphi,\nabla^2\varphi]=\frac{\partial\varphi}{\partial x}\frac{\partial\nabla^2\varphi}{\partial y}-\frac{\partial\varphi}{\partial y}\frac{\partial\nabla^2\varphi}{\partial x}$$

is the Jacobian between the electrostatic potential φ and the vorticity $\zeta=\nabla^2\varphi$. It is also known that Poisson-bracket or vector nonlinearity of Eq. (1) facilitates the formation of robust dipole vortices.[1] Recently, there have been numerous studies of this type of nonlinearity and vortex dynamics.[2,3] However, a more comprehensive theory includes the nonlinearity as given in Eq. (1), together with KdV or scalar type nonlinearity, which was first introduced by Petviashvili[4] in the case of drift waves. Due to the presence of the scalar nonlinearity, the dipole vortex is no longer an exact solution. Here we investigate the question: How does this scalar nonlinearity affect the evolution of the dipole vortex? We will show numerically that even a small amount of scalar nonlinearity can have important consequences for the vortices.

Hydrodynamic experiments of Soviet scientists[5,6] have shown that there is a rather rapid transition from a dipole vortex pair to isolated monopole vortices. This transition we argue arises as a result of competition between the vector and scalar nonlinearities. From the analogy between the Coriolis force dynamics describing Rossby waves in rotating hydrodynamics and the Lorentz force dynamics describing drift waves in a magnetized inhomogeneous plasma, we expect that the splitting process of the dipole vortex into monopoles should also occur in a plasma for drift solitary waves. It is, therefore, worthwhile to numerically sim-

ulate the dynamics of dipole vortices incorporating a small scalar nonlinearity, and thus to investigate how the scalar nonlinearity splits up the dipole.

This paper is organized as follows: in Sec. II, we give the equation of the simulation model and present its conservation laws. Exact monopole solutions are presented in Sec. III. In Sec. IV we describe how the dipole vortex splits up and give simulation results on the evolution when the dipole vortex pair is the initial state. In Sec. V we discuss the stability of the positive and negative monopoles that split off of the dipole vortex. Section VI gives a summary and the conclusions.

II. Model Equation and Conservation Laws

We consider a plasma in a uniform external magnetic field in the z-direction. The gradients in plasma density $\frac{d\ell n\, n_0}{dx}$ and the electron temperature $\eta_e = d\ell n\, T_e / d\ell n\, n_e$ are along the x-axis, the diamagnetic drift velocity $v_d = -(cT_e/eB_0)\frac{d\ell n\, n_0}{dx}$ is along the y-axis. To describe the dynamics of the potential drift waves in such a plasma, we consider the contribution of the electron and ion polarization drifts to the density equation and we use the condition of quasineutrality of perturbations. We thus derive the following model equation

$$(1-\nabla^2)\frac{\partial \varphi}{\partial t} + v_d \frac{\partial \varphi}{\partial y} + \alpha\varphi\frac{\partial \varphi}{\partial y} + [\nabla^2\varphi, \varphi] = 0 \tag{2}$$

where $\alpha = v_d\eta_e = \frac{\rho_s}{r_{T_e}}$, $\varphi = \frac{e\phi}{T_e}$, ϕ is electric potential, ρ_s is the ion Larmor radius with electron temperature T_e, r_{T_e} is the characteristic length of plasma inhomogeneity, space and time variables are normalized by ρ_s and the ion cyclotron frequency, respectively.

Rossby waves in rapidly rotating shallow neutral fluids also satisfy Eq. (2) with the scalar nonlinearity arising from variations in the depth of the fluid and $[\nabla^2\varphi, \varphi]$ arising from the convective acceleration $\mathbf{v}\cdot\nabla\mathbf{v}$ of the fluid.

For weakly inhomogeneous plasma, ρ_s/r_{T_e} is small compared to unity and thus the scalar nonlinearity, i.e. the α term is typically neglected, whereupon Eq. (2) reduces to Eq. (1).

If we keep the scalar nonlinearity, then the dipole vortex is no longer an exact solution. As mentioned above (and shown below) this term splits the dipole vortex into two monopoles of opposite sign.

Consider now the conservation laws of Eq. (2) after the scalar nonlinearity is added.

1. Equation (2) can be rewritten as

$$\frac{\partial \varphi}{\partial t} + \nabla \cdot \left[-\frac{\partial \nabla \varphi}{\partial t} + \left(v_d \varphi + \frac{\alpha \varphi^2}{2} \right) \hat{y} + (\nabla \varphi \times \hat{z}) \nabla^2 \varphi \right] = 0 \, . \tag{3}$$

Equation (3) represents the conservation of mass in the two-dimensional system.

2. Multiplying Eq. (2) by φ, we derive the following equation

$$\frac{\partial \varepsilon}{\partial t} + \nabla \cdot \left[\left(\frac{1}{2} v_d \varphi^2 + \frac{1}{3} \alpha \varphi^3 \right) \hat{y} - \varphi \nabla \frac{\partial \varphi}{\partial t} - \nabla^2 \varphi \left(\hat{z} \times \nabla \frac{\varphi^2}{2} \right) \right] = 0 \tag{4}$$

where

$$\varepsilon(x, y, t) = \frac{1}{2} \left[\varphi^2 + (\nabla \varphi)^2 \right]$$

is the local energy density. Equation (4) gives the energy conservation law.

3. Multiplying Eq. (2) by x, we get another constant of motion,

$$\begin{aligned} \frac{\partial (x\varphi)}{\partial t} \; + \; & \nabla \cdot \left[\left(\frac{\partial \varphi}{\partial t} \right) \hat{x} + \left[x \left(v_d \varphi + \frac{\alpha \varphi^2}{2} \right) + \frac{|\nabla \varphi|^2}{2} \right] \hat{y} - \frac{\partial \varphi}{\partial y} \nabla \varphi \right. \\ - \; & \left. \frac{\partial (x \nabla \varphi)}{\partial t} + x (\nabla \varphi \times \hat{z}) \nabla^2 \varphi \right] = 0 \end{aligned} \tag{5}$$

giving the conservation law for the x coordinate for the center of mass.

The above three constants of motion are used in our simulation to observe the accuracy of the numerical integration of Eq. (2).

We also notice that the potential entrophy $U = \langle (\nabla \varphi)^2 + (\nabla^2 \varphi)^2 \rangle$ is not conserved for $\alpha \neq 0$.

III. Exact Monopole Solutions

In order to interpret our results we first present exact monopole solutions to Eq. (2). Assuming a travelling steady state solution $\varphi = \varphi(x, y - ut)$, Eq. (2) becomes

$$-u(1-\nabla^2)\frac{\partial\varphi}{\partial y} + v_d\frac{\partial\varphi}{\partial y} + \alpha\varphi\frac{\partial\varphi}{\partial y} + [\nabla^2\varphi, \varphi] = 0 \ . \tag{6}$$

For axisymmetric monopoles, $\varphi(r,\theta) \to \varphi(r)$ and $[\varphi(r),\ \nabla^2(\varphi(r))] = 0$, leaving

$$\frac{1}{r}\frac{d}{dr}\left(r\frac{d\varphi}{dr}\right) = 4k^2\varphi - \frac{\alpha}{2u}\varphi^2 \tag{7}$$

where

$$k^2 = \frac{1}{4}\left(1 - \frac{v_d}{u}\right) \ . \tag{8}$$

Defining $\varphi = \varphi_m\psi(\xi)$, where $\xi = kr$, Eq. (7) becomes the following in terms of ψ:

$$\frac{d^2\psi}{d\xi^2} + \frac{1}{\xi}\frac{d\psi}{d\xi} = 4\psi - 6\gamma\psi^2 \ . \tag{9}$$

Here we have set

$$\varphi_m = \frac{12\gamma u k^2}{\alpha} \tag{10}$$

where γ is a constant that remains to be determined.

We compare Eq. (9) to the analogous equation for one-dimensional solitary drift waves that are solutions of the regularized long-wave equation,[7,8]

$$\phi_t - \phi_{yyt} + v_d\phi_y + \alpha\phi\phi_y = 0 \ . \tag{11}$$

This equation is the one-dimensional restriction of Eq. (2). Inserting $\varphi = \varphi_m\psi\left(k(y-ut)\right)$ yields

$$\frac{d^2\psi}{d\xi^2} = 4\psi - 6\psi^2 \tag{12}$$

where $\xi \equiv k(y-ut)$, $k^2 = \frac{1}{4}(1 - v_d/u)$ and $\varphi_m = 12uk^2/\alpha$. For $k^2 > 0$ Eq. (12) possesses the well-known solution $\psi = \mathrm{sech}^2\xi$.

It is apparent that the monopole speed-width relation, Eq. (8), is identical with that for the one-dimensional case. But, the amplitude relation of Eq. (10) differs by the presence of γ, which also occurs in Eq. (9), the equation for the shape of the monopole. This later equation, together with the boundary conditions

$$\frac{d\psi}{d\xi}(\xi = 0) = 0 \qquad , \qquad \lim_{\xi \to \infty} \frac{1}{\psi} \frac{d\psi}{d\xi} = -2 \tag{13}$$

and the condition $\psi(\xi = 0) = 1$ defines a nonlinear eigenvalue problem for γ. Numerically we obtain $\gamma = 1.5946$; the shape of the eigenfunction defined by this procedure is shown in Fig. 1a. In our computations we set γ to unity and then vary the value of ψ and $d\psi/d\xi$ at large values of ξ, consistent with the second equality of Eq. (13), until $d\psi(\xi = 0)/d\xi = 0$ is achieved. This yields $\psi(\xi = 0) = \gamma$. Scaling by γ then gives the desired result.

The above calculation is only valid for $k^2 > 0$, which implies $u > v_d$ or $uv_d < 0$. In light of Eq. (10) positive velocity monopoles have $\varphi_m > 0$. These are referred to as anticyclones. The negative ($uv_d < 0$) velocity monopoles have negative φ_m and are referred to as cyclones. In the case $k^2 < 0$ neither the two-dimensional Eq. (9) nor the one-dimensional equation Eq. (12) possess exponentially localized solutions. When $k^2 < 0$, the wave structure propagates with $0 < u < v_d$, and, in two dimensions, is a weakly localized oscillatory (radiation) solution where the amplitude decays as $\xi^{-1/2}$.

In Fig. 1b we plot solutions to Eq. (9). All of these solutions have $d\psi(\xi = 0)/d\xi = 0$. For $\psi(\xi = 0) > \gamma$, the solution diverges to $-\infty$. Solutions with $0 < \psi(\xi = 0) \lesssim \gamma$ are homoclinic to $\psi = 2/3$. These nonlinear oscillatory solutions are the radiation solutions mentioned above and describe finite amplitude cylindrically symmetric waves propagating with speed u such that $0 < u < v_d$. Mathematically, these wave solutions can be "pulled down" by the following symmetry relation:

$$\overline{\varphi}(-k^2; r, \theta) = \varphi(k^2; r, \theta) - \frac{8uk^2}{\alpha}.$$

If φ solves $\nabla^2\varphi - k^2\varphi + \alpha\varphi^2/2u = 0$, then $\overline{\varphi}$ solves $\nabla^2\overline{\varphi} + k^2\overline{\varphi} + \alpha\overline{\varphi}^2/2u = 0$. Thus, Fig. 1b compactly displays both the solitary wave and radiation solutions.

Additional symmetries of Eqs. (1) and (2) are as follows. For every solution of Eq. (1) $\varphi(x,y,t)$ there is a solution $-\varphi(-x,y,t)$ (i.e., Eq. (1) has the symmetry $\varphi(x,y,t) \rightarrow -\varphi(-x,y,t)$.) This symmetry is lost when the scalar nonlinearity is added to the equation, Eq. (2). This antisymmetry in x is the symmetry property possessed by the dipole vortex solution given in Eq. (14). When the scalar nonlinearity is added there is no symmetry for a given α, but for the two different equations with α and $-\alpha$ there is the symmetry relation

$$\varphi(-\alpha; x, y, t) = -\varphi(\alpha, -x, y, t) \ .$$

Thus a small, finite α lifts a degeneracy in the $\alpha = 0$ equation.

IV. Dipole Vortex Splitting into Monopoles

The dipole vortex solution possessed in the absence of scalar nonlinearity is given by

$$\varphi = \begin{cases} \left[-\dfrac{k^2 r_0}{p^2 r} \dfrac{J_1(pr)}{J_1(pr_0)} + \left(1 + \dfrac{k^2}{p^2}\right) \right] ur\cos\theta & (r < r_0) \\ ur_0 \dfrac{K_1(kr)}{K_1(kr_0)} \cos\theta & (r > r_0) \end{cases} \tag{14}$$

where $r^2 = x^2 + (y - ut)^2$, $u = v_d/(1 - k^2)$, $x = r\cos\theta$, and $y = r\sin\theta$. The parameters p and k are related by

$$\frac{1}{kr_0}\frac{K_2(kr_0)}{K_1(kr_0)} = -\frac{1}{pr_0}\frac{J_2(pr_0)}{J_1(pr_0)} \ ,$$

which follows from continuity of the flow velocity $\mathbf{v} = \hat{z} \times \nabla\varphi$ across $r = r_0$.

Previous simulation studies of Eq. (2) by Mikhailovskaya,[9] with Eq. (14) as the initial state, indicate that when α is large enough, the dipole vortex rapidly separates into pieces moving in opposite directions away from their initial positions. The radius of anticyclones

($\varphi > 0$) increases slightly, but the amplitude decreases and approaches a circular shape. Cyclones ($\varphi < 0$), are observed to gradually decay into small vortices that finally disappear.

We find a somewhat different result. From our calculations and simulations, we conclude that the dipole vortex pair splits into *both* the anticyclone and the cyclone monopoles, which maintain their integrity.

In order to interpret our results and to understand the discrepancy with Mikhailovskaya we use the amplitude and width-speed relations of Sec. III. From Eqs. (8) and (10) we obtain the following speed for anticyclones:

$$u = v_d + \frac{\alpha|\varphi_m|}{3\gamma}, \tag{15}$$

while for cyclones, $\varphi_m < 0$, and the speed is given by

$$u = v_d - \frac{\alpha|\varphi_m|}{3\gamma}, \tag{16}$$

where exponential localization requires $\alpha|\varphi_m| > 3\gamma$. The anticyclone and cyclone propagate with different speeds, the relative speed is $u_+ - u_- = \alpha|\varphi_m^+|/(3\gamma) + \alpha|\varphi_m^-|/(3\gamma)$. This result explains why the initial dipole vortex pair will split apart into two isolated monopoles with opposite signs. The time scale for the breakup of the dipole vortex can be estimated from

$$\Delta t \sim r_0/(\alpha|\varphi_m|)\ . \tag{17}$$

This relation is observed by our simulations.

To solve Eq. (2), we use a uniform grid over k_x and k_y in 85×85 **k**-space with 3612 complex $\varphi_{\mathbf{k}}(t)$ modes using the 128×128 FFT. The equations are solved using high order Runge-Kutta time stepping and the Fourier transformation $(x, y) \leftrightarrow (k_x, k_y)$ at each time step. The constants of motion in Sec. II are used to monitor the accuracy of the numerical integration of Eq. (2). They, in fact, remain constant within the fraction 10^{-3} during the simulation experiments. The initial perturbation $\varphi(x, y, 0)$ is taken to be the dipole vortex

given in Eq. (14) with $r_0 = 6(\rho_s)$, $u = 2v_d$ and $v_d = c_s\rho_s/r_n$. Typical simulations use 20 minutes CPU on the CRAY-II for $\Delta t = 100r_n/c_s$.

We studied two cases with $\alpha = 0.01$ and $\alpha = 0.1$, and observed the same results, except that the time scale of breakup for $\alpha = 0.01$ is about 10 times larger than that for $\alpha = 0.1$.

Figure 2 shows the streamlines $\varphi(x, y, t) =$ const. at times $tc_s/r_n = 0$, 2, 10, and 100. Observe that at $tc_s/r_n = 10$, the initial dipole vortex splits into the two completely isolated monopoles and the two monopoles approach circular shape. We also observed that the amplitudes of the vortices increases slightly, but the radius of both the vortices does not change much until $t \simeq 30$. The observed speed of the anticyclone is $u \simeq 2.0v_d$ and that of the cyclone is $u \simeq -0.3v_d$.

Moreover, when we turn off the vector nonlinearity and redo the same experiment, we observed that the radius of the cyclone decreases significantly very rapidly and its amplitude increases a significant amount and then forms a very localized monopole vortex or solitary wave while the radius of the anticyclone doesn't change much and its amplitude increases slightly. The evolution of the processes are illustrated by Fig. 3. In the case of an anticyclone, this result appears to be in accordance with the simulation studies of Eq. (2) made in Ref. 10 in the long wavelength limit.

Now we consider whether the anticyclone and cyclones can naturally evolve from the one-dimensional solitary waves described by Eq. (12).

For $k_x \approx 0$, we know that Eq. (2) has the solitary wave solution given by Petviashvili,[4] Meiss and Horton[7] and Morrison et al.[8]

$$\varphi = \frac{3}{\alpha}(u - v_d)\mathrm{sech}^2\left[\frac{1}{2}\left(1 - \frac{v_d}{u}\right)^{1/2}(y - ut)\right] , \tag{18}$$

where u, as before, is the speed.

However, the one-dimensional solitary wave is unstable to a finite k_x filamentation instability shown as follows. Taking Eq. (18) as the initial condition, we find that the computer

solution of Eq. (2) evolves into the two-dimensional, nearly circularly symmetric monopole vortices. The results are shown in Fig. 4.

The solution (18) is possible only when $u > v_d$ or $v_d u < 0$. For $u > v_d$, we find that the positive solitary wave eventually evolves into two-dimensional anticyclones, as shown in Fig. 4. For $u < 0$, we also find that the negative solitary wave,

$$\varphi = -\frac{3}{\alpha}(|u| + v_d)\mathrm{sech}^2\left(\frac{\sqrt{1+\frac{v_d}{|u|}}}{2}y\right) \tag{19}$$

evolves into two-dimensional cyclones with $k_x \sim k_y$. From Eq. (16), we can see that $\varphi_m < 0$ occur for $\alpha|\varphi_m|/3\gamma > v_d$ where $u < 0$. With Eq. (19) as initial data, we find that cyclones evolve out of the one-dimensional negative solitary wave.

V. Stability of Cyclone and Anticyclone

As noted in Sec. IV, Mikhailovskaya[9] did some simulation studies of Eq. (2). Her results indicate that when α is large enough, that is, the scalar nonlinearity is dominant, the dipole vortex rapidly separates with monopoles moving in opposite directions away from their initial positions. The radius of anticyclones ($\varphi > 0$) increase slightly. The amplitude decreases and it approaches a circular shape, but cyclones ($\varphi > 0$), she finds, gradually decay into small vortices and finally disappear. In general, we find a different result, both theoretically and numerically.

Now we ask if the cyclone will disappear eventually; in other words, if the cyclone can be the solution of Eq. (2).

From Sec. III the solitary wave solution (7) of Eq. (2) does exist, from (8) and (10) with

$$\varphi = \left[\frac{3\gamma}{\alpha}(u - v_d)\right]\psi(kr) \tag{20}$$

and $r = [x^2 + (y - ut)^2]^{1/2}$. So for $u > v_d$, we get a solitary solution for positive amplitude. For $u < 0$ we get for negative amplitude, and positive k^2 provided $\alpha|\varphi_m| > 3\gamma v_d$.

This means that both the cyclones and anticyclones can exist and stay stable in the system after the initial dipole vortex pair breaks up if the amplitude φ_m of the dipole pair is large enough so that $\alpha|\varphi_m| > 3\gamma v_d$. This condition requires a substantial amplitude and energy for the solitary wave to form the cyclone.

We, therefore, think that the disappearance of cyclone observed in the experiments[5,6] and in the numerical simulation[9] is probably due to too small of an amplitude so that $\alpha|\varphi_m| < 3\gamma v_d$ for which it follows that $0 < u < v_d$. This is a regime of radial outgoing wave solitons which dissipate away the cyclone. This type of radiation damping is important for drift waves in plasmas with magnetic shear which we now briefly discuss. In the rotating fluid experiments the radiation damping would appear as a wake of Rossby waves that disperse the energy in the vortex core.

The most important inhomogeneity in a plasma is typically the magnetic shear $S = r_n/L_s$, which can cause the monopoles to decay.[2] The drift wave vortex has local $k_\| = 0$, but due to the magnetic shear away from the core $k_\| = k_y(x/L_s)$. Taking into account the coupling to the parallel ion acceleration $\dot{v}_\| = -(e/m_i)\hat{b}\cdot\nabla\Phi$ leads to the shear induced ion acoustic term in Eq. (6)

$$-u(1-\nabla^2)\frac{\partial\varphi}{\partial y} + v_d\frac{\partial\varphi}{\partial y} + \frac{S^2x^2}{u}\frac{\partial\varphi}{\partial y} + \alpha\varphi\frac{\partial\varphi}{\partial y} + [\nabla^2\varphi,\varphi] = 0\ . \tag{21}$$

In the small amplitude region exterior to the vortex core the wave field is given by

$$\partial_x^2\varphi_{k_y}(x) + \left(-1 - k_y^2 + \frac{v_d}{u} + \frac{S^2x^2}{u^2}\right)\varphi_{k_y}(x) = 0\ , \tag{22}$$

with

$$\varphi(x,y,t) = \int dk_y\varphi_{k_y}(x)e^{ik_y(y-ut)}.$$

For $uv_d < 0$ or $u > v_d$, Eq. (22) has turning points at $x = \pm x_T$ where $x_T^2 = u^2(1 + k_y^2 -$

$v_d/u)/S^2$. The wave spectrum for $x^2 > x_0^2$ is

$$\varphi_{k_y}(x) = \begin{cases} A_{k_y} Q(x)^{-1/4} \exp\left(i \int_{x_T}^{x} Q^{1/2}(x')dx'\right) & x > x_T \\ A_{k_y}(-Q(x))^{-1/4} \exp\left(-\int_{x_T}^{x}(-Q)^{1/2}dx' - \frac{i\pi}{4}\right) & x_0 < x < x_T \end{cases} , \tag{23}$$

where $Q(x) = S^2x^2/u^2 - k^2 - k_y^2$ and x_0 is the vortex core at $kx_0 \simeq 1$. We note that $\int_{x_T}^{x} Q^{1/2}(x')dx' \simeq Sx/2u^2$ for $x \gg x_T$ describing the outgoing radiation and that $\int_{x_T}^{x}(-Q)^{1/2}dx'$ $\simeq -\int_0^{x_T}(-Q)^{1/2}dx' + (k^2+k_y^2)^{1/2}x$, where the tunneling phase is $\int_0^{x_T}(-Q)^{1/2}dx = (\pi u/4S)(k^2+$ $k_y^2)$ for $x < x_T$.

The branch in Eq. (23) is chosen to satisfy outgoing energy boundary conditions with $\omega = k_y u$ and the stationary phase condition $\partial/\partial\omega(Sk_yx^2/2\omega + \omega t) = 0$, given the group velocity $x^2 = 2\omega^2 t/(k_y S) = (2k_y u^2/S)t$. In the presence of shear, the exterior vortex ($\xi \gtrsim 1$) solution

$$\varphi(x,y,t) = \frac{B}{(kr)^{1/2}} e^{-kr} \simeq \frac{3.1}{(kx)^{1/2}} e^{-kx - \frac{k(y-ut)^2}{2x}} \tag{24}$$

connects to the wave field (23) determining its amplitude $A(k_y)$. Taking the Fourier transform of (24), we obtain

$$A(k_y) = \frac{B(2\pi)^{1/2}(k^2+k_y^2)^{1/2}}{k} e^{i\pi/4 - \frac{\pi|u|}{4S}(k^2+k_y^2)} . \tag{25}$$

The outgoing wave propagation given by the connection of Eq. (24) to Eq. (23) leads to the decay of the total vortex energy E_v. Integrating the energy balance Eq. (4) over $\int_{-\infty}^{+\infty} dy$ and $\int_{-L}^{+L} dx$ and using Eq. (23) to evaluate the outgoing wave energy flux gives the rate of decay of vortex energy

$$\begin{aligned} \frac{dE_v}{dt} &= \int_{-L}^{+L} dx \int_{-\infty}^{+\infty} dy \frac{\partial \varepsilon}{\partial t} = u \int_{-\infty}^{+\infty} dk_y \; i \; k_y \left[\varphi_{k_y}^*(x)\partial_x\varphi_{k_y}(x) - \varphi_{k_y}(x)\partial_x\varphi_{k_y}^*(x)\right] \\ &\simeq -uS \int_0^{\infty} dk_y k_y |A_{k_y}|^2 . \end{aligned} \tag{26}$$

Using formula (25) for A_{k_y} we obtain the shear induced vortex decay rate

$$\frac{dE_v}{dt} = -\frac{4\pi S B^2}{k^3} \exp\left(\frac{-\pi|u|k^2}{2S}\right) \tag{27}$$

valid for $k^2 > 0$. Thus the shear damping is exponentially small provided the speed u is not too close to the wave propagation domain $0 \leq u \leq v_d$. In Eq. (27) $B \simeq 3.1$, computed from the unperturbed solitary vortex.

The theory for the effect of inhomogeneity due to magnetic shear in Eqs. (21)–(27) is based on the assumption that for strong vortices, the inhomogeneity causes a leakage of wave energy from the vortex core, but does not strongly alter the interior solution. At some stronger level of inhomogeneity the core of the vortex is perturbed, and non-perturbative solutions of the effect of inhomogeneity are required. Work is in progress for such nonperturbative nonlinear vortex solutions. Recent simulation studies by Carnevale *et al.*[11] for the effect of topography on monopole and dipole vortices show perturbative as well as destructive effects from inhomogeneities. Carnevale *et al.* presents simulations with topography (linear inhomogeneities) causing the dipole to split up into monopole vortices.

VI. Summary and Conclusions

Analytical and numerical studies on the effect of scalar nonlinearity on the evolution of dipole vortex solutions of the nonlinear drift wave–Rossby wave equation are reported. The study shows that the lifetime of the dipole drift vortices depends not only on the viscosity, but also on the magnitude of the scalar nonlinearity. For plasmas, the magnitude of the scalar nonlinearity is associated with a gradient of the plasma temperature,[4] η_e, in the field of a drift wave and is described by the parameter $\alpha = \eta_e \rho_s / r_n$. In the Rossby waves, the scalar nonlinearity arises from the variation of the depth of the fluid with wave amplitude, as in the classical KdV equation for shallow water waves. The dipole lifetime scale is estimated from $\tau \sim r_0 / \alpha \varphi_m$, where φ_m is a measure of vortex amplitude. We show that both the anticyclone ($\varphi > 0$) and cyclone ($\varphi < 0$) exist and do not disappear after the dipole vortex pair breaks up, in apparent contrast to the report of Mikhailovskaya,[9] who argues that the cyclone vortex disappears. We note, however, that there is a critical amplitude for the formation of the

cyclone which is probably not satisfied in her simulation.

The question of the existence of the cyclone solution is important for the interpretation of the rotating water tank experiments. In the early experiments of Antipov *et al.* ,[5,6] only anticyclones were reported to be long-lived vortices. In the work of Antonova *et al.* [12] with a larger tank, it is reported that both cyclones and anticyclones are formed. We suggest that cyclones, although requiring sufficient amplitude to form, are a natural solution of the nonlinear drift wave–Rossby wave equation. The cyclones may be especially important for anomalous transport because of their low propagation velocity.

Acknowledgments

The author gratefully acknowledges the work of Lee Leonard during the course of this investigation. The work was supported by the U.S. Department of Energy contract #DE-FG05-80ET-53088.

References

1. M. Makino, T. Kamimuya, and T. Tanuiti, J. Phys. Soc. Japan **50**, 980 (1981).

2. J.D. Meiss and W. Horton, Phys. Fluids **26**, 990 (1983).

3. W. Horton, *Drift Wave Vortices and Anomalous Transport*, Univ. of Texas IFSR #312, (1988).

4. V.I. Petviashvili, Fiz. Plazmy **3**, 270 (1977) [Sov. J. Plasma Phys. **3**, 150 (1977)].

5. S.V. Antipov, M.V. Nezlin, V.K. Rodionov, V.N. Snezhkin, and A.S. Trubnikov, Zh. Eksp. Teor. Fiz. **84**, 1357 (1983), [Sov. Phys. JETP **57**, 786 (1983)].

6. S.V. Antipov, M.V. Nezlin, E.N. Snezhkin, and A.S. Trubnikov, Zh. Eksp. Teor. Fiz. **82**, 145 (1982), [Sov. Phys. JETP **55**, 85 (1982)].

7. J.D. Meiss and W. Horton, Phys. Rev. Lett. **48**, 1362 (1982) and Phys. Fluids **25**, 1838 (1982).

8. P.J. Morrison, J.D. Meiss, and J.R. Cary, Physica **IID**, 324 (1984).

9. L.A. Mikhailovskaya, Fiz. Plazmy **12**, 879 (1986), [Sov. J. Plasma Phys. **12**, 507 (1986)].

10. V.P. Pavlenko and V.B. Tazanov, Sov. J. JETP **64**, 304 (1986 [Zh. Eksp. Teor. Fiz. **91**, 517 (1986)].

11. G.F. Carnevale, G.K. Vallis, R. Purini, and M. Briscolini, J. of Fluid Dynamics (to be published).

12. R.A. Antonova, B.P. Zhvaniya, D.G. Lominadze, D.I. Nanobashivili, and V.I. Petviashivili, Sov. Phys. JETP Lett. **37**, 651 (1983) [Pisma Zh. Eksp. Teor. Fiz. 545 (1983)].

Figure Captions

1. (a) Plot of the solitary wave solution of Eq. (9). (b) Solutions of Eq. (9) with $\psi'(0) = 0$. Curve 1 has $\psi(0) = 1.85$. Curve 2 has $\psi(0) = \gamma$ (as in 1(a)); it is homoclinic to zero: $\psi(r = \infty) = 0$. Curves 3 and 4 have $\psi(0) = 1.3$ and $\psi(0) = 0.1$, respectively. These, like all solutions with$\gamma > \psi(0) > 0$, are homoclinic to 2/3. When lowered by 2/3 these represent wave-like or radiation solutions. Curve 5 has $\psi(0) = -0.1$.

2. Splitting drift wave dipole vortex into monopoles with dipole radius $r_0 = 6\rho_s$, amplitude of scalar nonlinearity $\alpha = 0.1\,(\eta_e\rho_s/r_n)$, drift wave velocity $u = 2v_d$ ($v_d = 1$). At $t = 0$, (a) shows the contours for the exact dipole vortex solution to the Hasegawa-Mima–Rossby wave equation. The solid lines represent positive value of potential φ, and the dashed lines, negative value. The contours for φ have contour interval $\Delta\varphi = 4.0$.

3. Splitting dipole vortex without vector nonlinearity with everything the same as in Fig. 2, except that the vector nonlinear term in Eq. (2) is dropped out.

4. One-dimensional solitary wave traveling along the y-axis tears with finite k_x and forms two-dimensional solitary waves. (a) shows the contours for the initial 1-D solitary wave solution with $k_x = 0$. (b)-(c) show the reconnection of the flow lines to form four strong, nearly circular vortices. Here $\alpha = 0.1$ and $u = 2v_d$ for the initial 1-D solitary wave, Eq. (18).

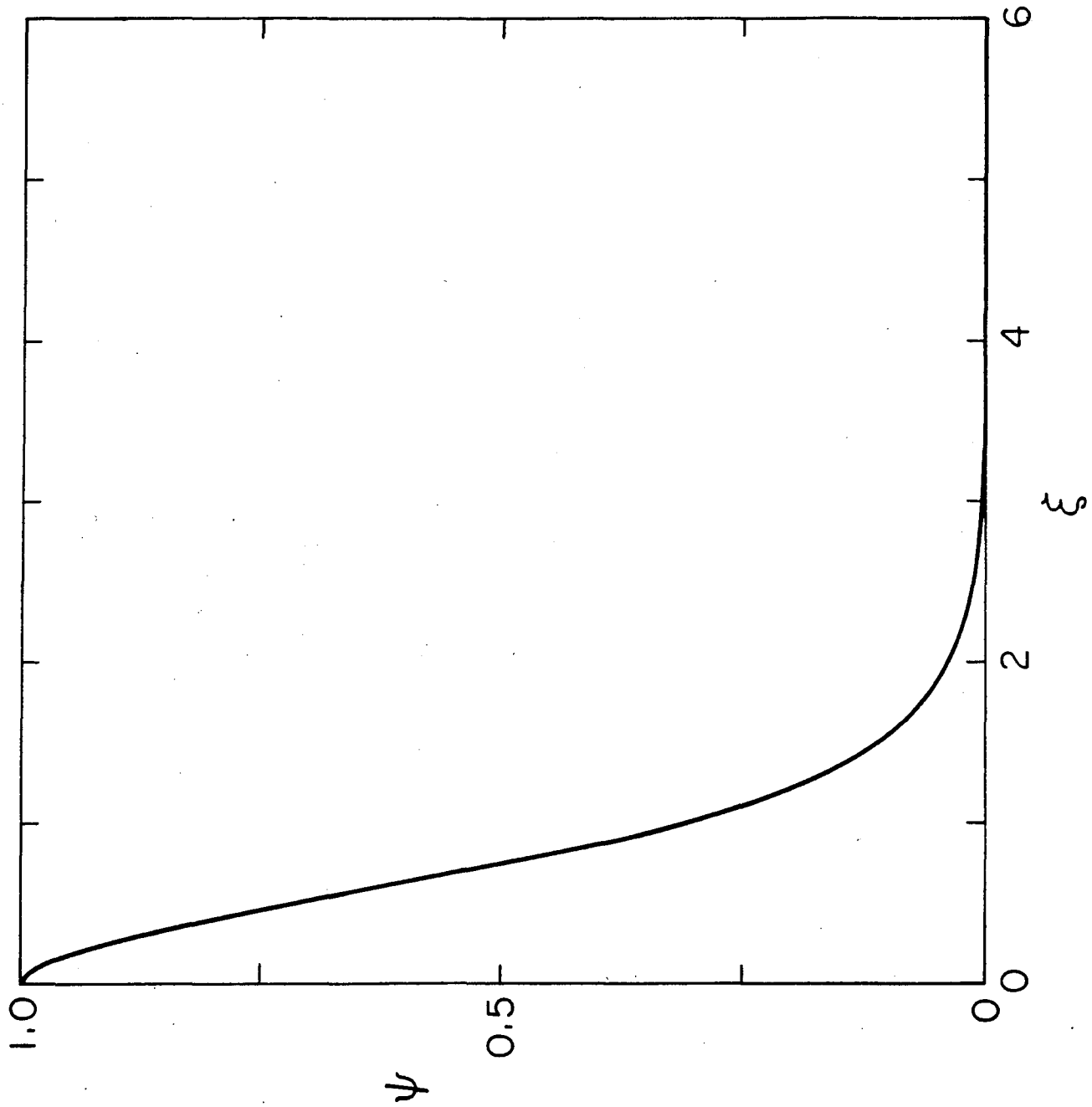

Fig. 1a

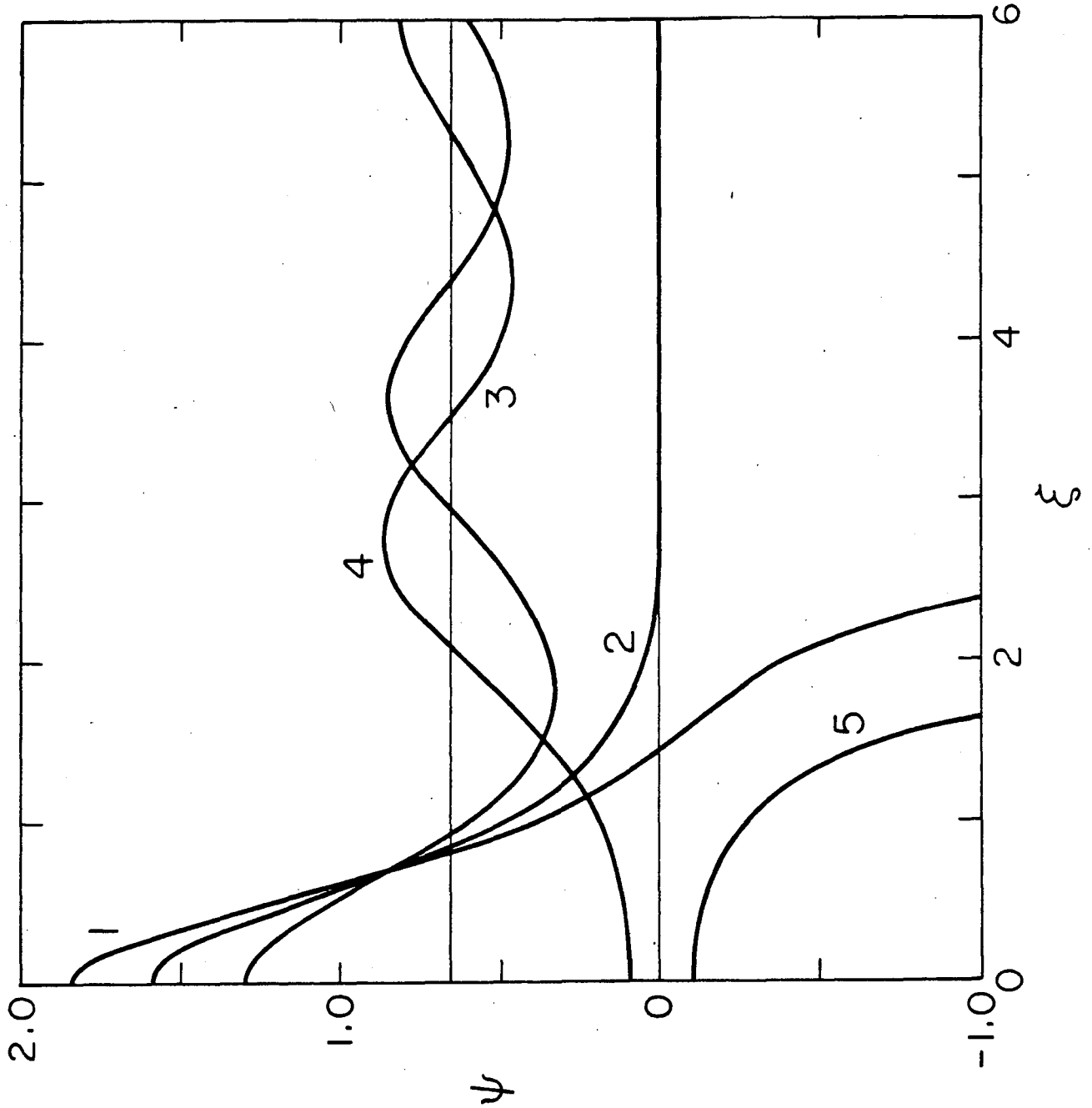

Fig. 1b

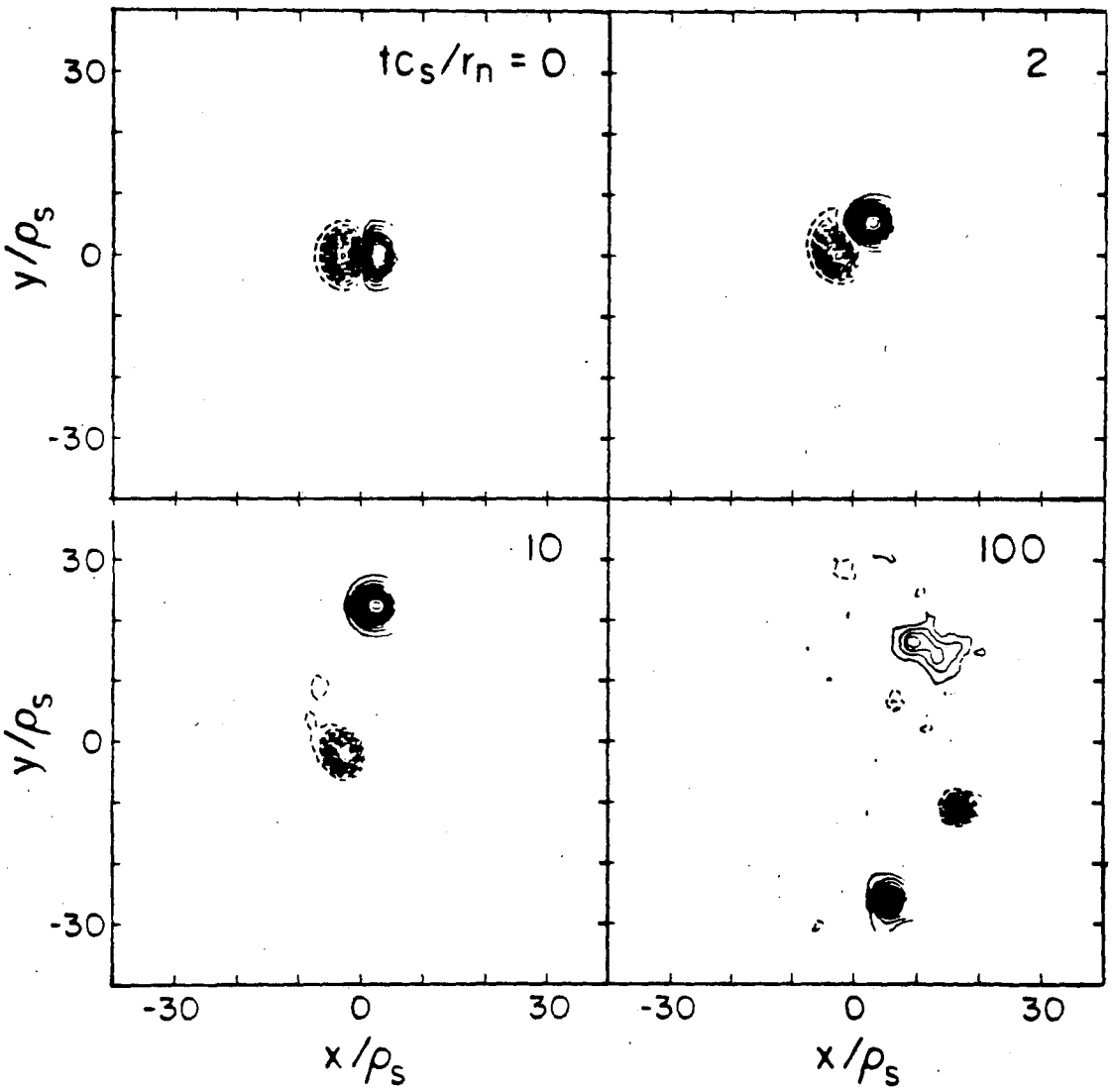

Fig. 2

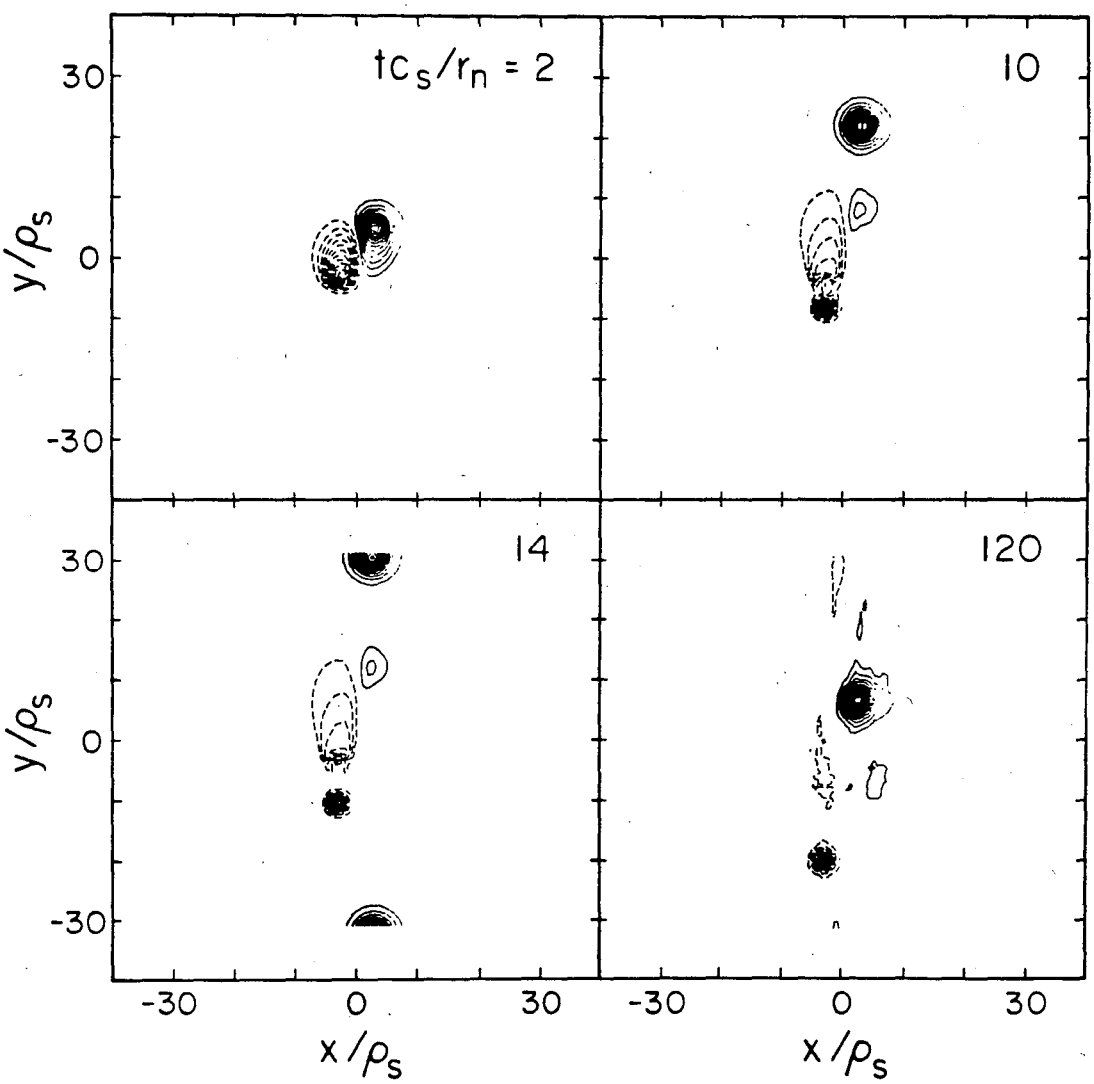

Fig. 3

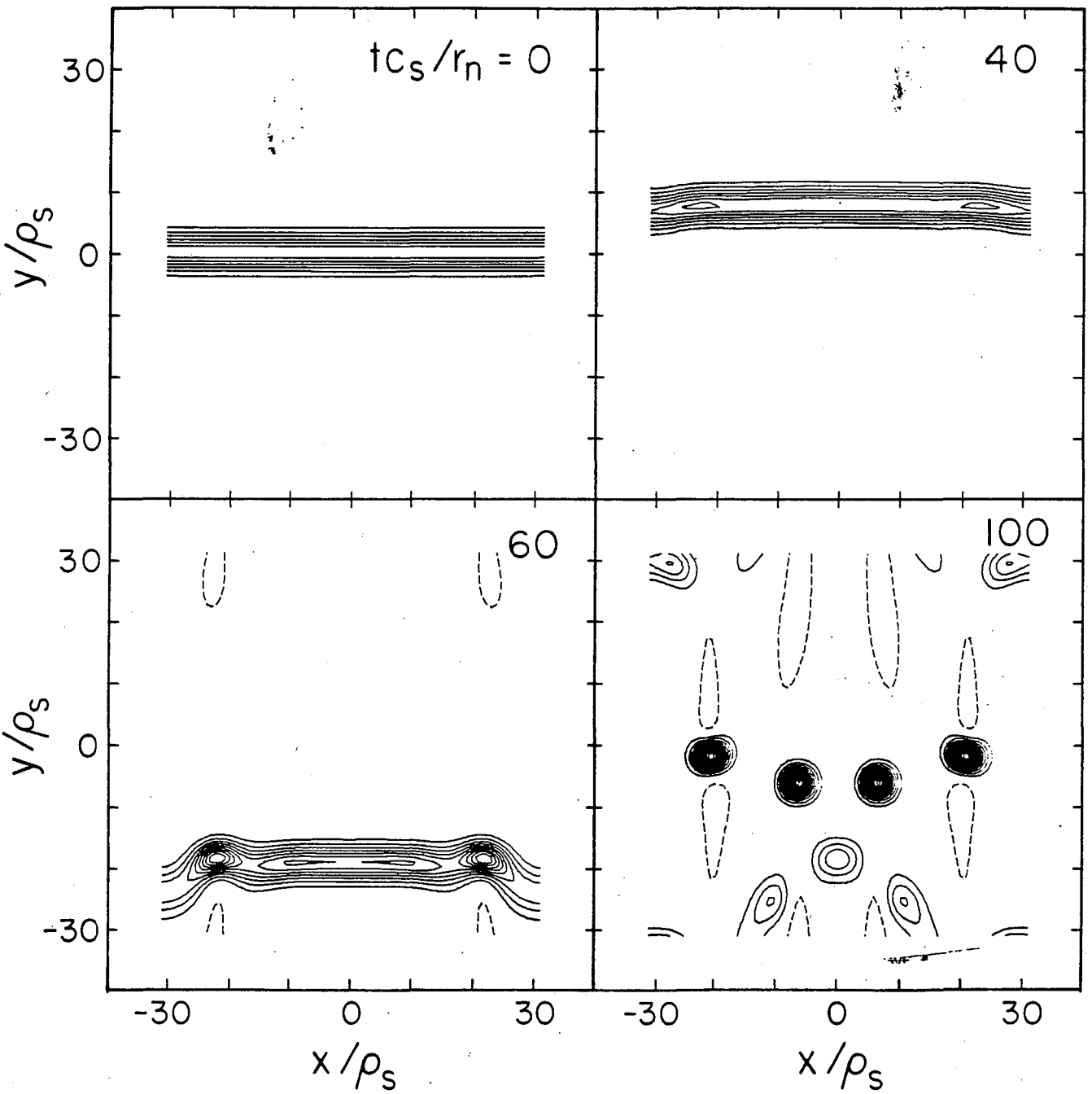

Fig. 4